# Supporting Information: Promising TMDC-like Optical and Excitonic Properties for $TiBr_2$ 2H Monolayer

André L. de O. Batista,[†] João Marcos Tomaz Palheta,[‡] Maurício J. Piotrowski,[*,‡] Celso R. C. Rêgo,[¶] Diego Guedes-Sobrinho,[§] and Alexandre C. Dias[*,‖]

[†]*Institute of Physics, University of Brasília, Brasília, DF, 70919-970, Brazil*

[‡]*Department of Physics, Federal University of Pelotas, PO Box 354, Pelotas, RS, 96010-900, Brazil*

[¶]*Karlsruhe Institute of Technology (KIT), Institute of Nanotechnology, Eggenstein-Leopoldshafen, Germany*

[§]*Chemistry Department, Federal University of Paraná, Curitiba, PR, 81531-980, Brazil*

[‖]*Institute of Physics and International Center of Physics, University of Brasília, Brasília, DF, 70919-970, Brazil*

E-mail: mauriciomjp@gmail.com; alexandre.dias@unb.br

## 1 Cohesion Energy

Here, using a cut off energy of 431.74 eV for the plane-wave basis function, for the isolated atoms, we place them inside an orthorhombic box with dimensions 21 Å, 22 Å, and 23 Å, considering only the Γ point, for the monolayer we use a **k**-mesh of $13 \times 13 \times 1$ and for the bulk **k**-mesh of $13 \times 13 \times 3$, which corresponds to a **k**-points density of 40 $Å^{-1}$ in each reciprocal lattice vector direction. All calculations were done with spin-polarized at the PBE level. The $TiBr_2$ 2H bulk atomic structure was optimized using the same monolayer protocol described in the manuscript. For isolated atoms, we obtained a total energy of $E_{Ti} = -4.767812$ eV for Ti

and $E_{Br} = -0.267355$ eV for Br, for $TiBr_2$ 2H bulk we obtained $E_{\text{bulk}} = -33.462375$ eV and for the $TiBr_2$ 2H monolayer we obtained $E_{\text{mono}} = -16.724246$ eV.

Thus, the $E_{\text{coh}}$ values for the $TiBr_2$ 2H monolayer ($E_{\text{coh}}^{\text{mono}}$) and for the bulk ($E_{\text{coh}}^{\text{bulk}}$) were calculated as follows:

$$E_{\text{coh}}^{\text{mono}} = \frac{E_{\text{mono}} - E_{\text{Ti free-atom}} - 2E_{\text{Br free-atom}}}{3} = -3.807 \text{ eV} , \quad (1)$$

and

$$E_{\text{coh}}^{\text{bulk}} = \frac{E_{\text{bulk}} - 2E_{\text{Ti free-atom}} - 4E_{\text{Br free-atom}}}{6} = -3.810 \text{ eV} . \quad (2)$$

The negative values obtained strongly support the argument for the stability of our systems. An alternative way to determine the formation energy involves using the enthalpy of formation ($\Delta H_{\text{f}}$). This method only requires estimating the total energies of chemical precursors along a specific synthesis route, as it is a state function. However, considering the numerous possible synthetic routes, such as those found in transition metal dichalcogenides[S1–S5], which can be based on top-down or bottom-up strategies, may not be feasible in every scenario.

## 2 Thermodynamic Properties

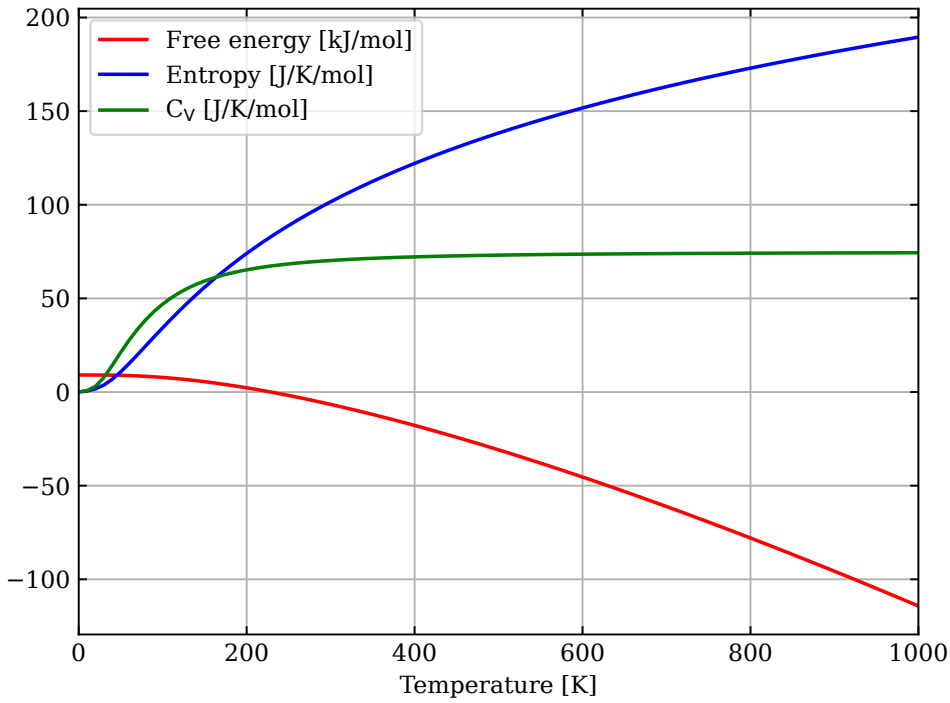


Figure S1: Thermodynamic Potentials: The Gibbs free energy (red curve), entropy (blue curve), and heat capacity at constant volume (green curve), for $TiBr_2$ 2H monolayer.

In Fig.S1, the Gibbs free energy reveals that the system exhibits favorable synthesis conditions for temperatures exceeding 200 K, suggesting the feasibility of obtaining our system at room temperature. This observation aligns with the trends observed in entropy and $C_V$ as depicted in Fig.S1.

## References

(S1) Kong, D.; Wang, H.; Cha, J. J.; Pasta, M.; Koski, K. J.; Yao, J.; Cui, Y. Synthesis of $MoS_2$ and $MoSe_2$ Films with Vertically Aligned Layers. **2013**, *13*, 1341–1347, DOI: 10.1021/nl400258t, PMID: 23387444.

(S2) Empante, T. A.; Zhou, Y.; Klee, V.; Nguyen, A. E.; Lu, I.-H.; Valentin, M. D.; Naghibi Alvillar, S. A.; Preciado, E.; Berges, A. J.; Merida, C. S.; Gomez, M.; Bobek, S.;

Isarraraz, M.; Reed, E. J.; Bartels, L. Chemical Vapor Deposition Growth of Few-Layer $MoTe_2$ in the 2H, 1T′, and 1T Phases: Tunable Properties of $MoTe_2$ Films. *ACS Nano* **2017**, *11*, 900–905, DOI: 10.1021/acsnano.6b07499.

(S3) Chen, Y.; Cui, P.; Ren, X.; Zhang, C.; Jin, C.; Zhang, Z.; Shih, C.-K. Fabrication of $MoSe_2$ Nanoribbons via an Unusual Morphological Phase Transition. *Nat. Commun.* **2017**, *8*, 15135, DOI: 10.1038/ncomms15135.

(S4) Sharma, P.; Kumar, A.; Bankuru, S.; Chakraborty, J.; Puravankara, S. Large-scale surfactant-free synthesis of $WS_2$ nanosheets: an investigation into the detailed reaction chemistry of colloidal precipitation and their application as an anode material for lithium-ion and sodium-ion batteries. *New Journal of Chemistry* **2020**, *44*, 1594–1608, DOI: 10.1039/c9nj04662c.

(S5) Duraisamy, S.; Ganguly, A.; Sharma, P. K.; Benson, J.; Davis, J.; Papakonstantinou, P. One-Step Hydrothermal Synthesis of Phase-Engineered $MoS_2/MoO_3$ Electrocatalysts for Hydrogen Evolution Reaction. **2021**, *4*, 2642–2656, DOI: 10.1021/acsanm.0c03274.